C. Naumann, T. Kick, T. Methling, M. Braun-Unkhoff, U. Riedel, Ethene / Nitrous Oxide Mixtures as a Green Propellant to substitute Hydrazine: Reaction Mechanisms Validation, Int. J. Energetic Materials Chem. Prop. 19 (2020) 65-71.

The original publication is available at www.begellhouse.com

http://dx.doi.org/10.1615/IntJEnergeticMaterialsChemProp.2020028133/

isicp2018-23787

ETHENE / NITROUS OXIDE MIXTURES AS GREEN PROPELLANT TO SUBSTITUTE HYDRAZINE: REACTION MECHANISM VALIDATION

Clemens Naumann [1*], Thomas Kick [1], Torsten Methling [2], Marina Braun-Unkhoff [1], Uwe Riedel [1]

[1]*German Aerospace Center (DLR), Institute of Combustion Technology, Stuttgart, Germany*

[2]*Lund University, Department of Physics, Lund, Sweden*

*Address all correspondence to: clemens.naumann@dlr.de

Original Manuscript Submitted: 08/20/2018; Final Draft Received: MM/DD/YYYY

Reaction mechanism validation for nitrogen diluted ethane/nitrous oxide mixtures at stoichiometric conditions has been performed using ignition delay time measurements at p = 1, 4 and 16 bar as well as laminar flame speed measurements at p = 1 and 3 bar. The predictive capability of the public domain mechanism GRI 3.0 was improved considerably by adapting some reactions within the nitrogen-subsystem and optimizing the most sensitive reactions with respect to selected optimization targets, i.e. ignition delay time and selected laminar flame speed measurements, within the published error bounds.

KEY WORDS: *green propellants, hydrazine replacement, ethene, nitrous oxide fuel blends, premixed monopropellant, ignition delay time, laminar flame speed, validation, reaction mechanism*

1. INTRODUCTION

Hydrazine and hydrazine derivatives like monomethyl hydrazine (MMH) and unsymmetrical dimethyl hydrazine (UDMH) are used for spacecraft propulsion applications in various technological contexts despite their drawback of being highly toxic. Today, hydrazine consumption for European space activities is in the order of 2-5 tons per year. However, if the impact of the REACH (Registration, Evaluation, Authorisation and Restriction of Chemicals) regulation should come into full force in the upcoming years, hydrazine use in Europe will be severely restricted, although the propellant may remain available from other sources outside Europe. Nevertheless, green propellants for European space activities are an accepted challenge for research and for technology development. Similar to research programmes in the U.S. initiated by DARPA (see Tiliakos et al. (2001) or ADMG (2012)), DLR investigates the combustion properties of propellants like ethene/nitrous oxide mixtures that have the potential to substitute hydrazine or hydranzine/dinitrogen tetroxide in chemical propulsion systems (Werling et al. (2015), Werling et al. (2016), Werling et al. (2017)). Data from model combustors operated at DLR's rocket propulsion test site at Lampoldshausen (Germany) in combination with investigations of fundamental combustion properties provide valuable test cases to be analysed by CFD computations, thus gaining better insights to the specific design requirements of new rocket engines powered by green propellants.

For these reasons, this work deals with the measurement of ignition delay times and laminar flame speeds of ethane/nitrous oxide mixtures and its use for the validation of the reaction mechanism to support CFD combustor simulations. Ignition delay times of stoichiometric mixtures of C_2H_4/N_2O diluted 1:5 with nitrogen have been investigated behind reflected shock waves at initial pressures of $p_{nominal}$ = 1, 4, and 16 bar. Complementary, laminar flame speeds have been measured at a dilution of 1:2 with nitrogen at pressures ranging from

atmospheric up to 10 bar using a conical laminar premixed flame. Subsequently, the predictive capability of the public domain reaction mechanism GRI 3.0 from Smith et al. (2000) extended as proposed by Powell et al. (2009) and adapted with respect to high temperature dissociation reactions and collision enhancement factors of C_2H_4 and N_2O will be shown at the conditions tested. In addition, the results will be compared to an optimized version of the reaction scheme obtained using the linear transformation model (lin-TM) as developed for the optimization and reduction of chemical kinetic models by Methling et al. (2016).

2. EXPERIMENTAL SETUP

2.1 Ignition delay time experiments

The experiments were carried out in a shock tube with an internal diameter of 98.2 mm. It is divided by aluminium diaphragms into a driver section of 5.18 m and a driven section of 11.12 m in length. Driver and driven sections are separated by a small intermediate volume establishing a double-diaphragm operation. The driver section was loaded with mixtures of helium and argon controlled by Bronkhorst mass flow controllers to achieve tailored interface conditions. The driven section was pumped down to pressures below 10^{-6} mbar by a turbomolecular pump. Reactive gas mixtures were prepared manometrically in stainless steel storage cylinders, which were evacuated using a separate turbomolecular pump. Gases used were delivered by LINDE AG (N_2O: 99.999%, C_2H_4: 99.95%, diluent N_2: 99.9995% (ECD)). The shock speed was measured over three 200 mm intervals using four piezoelectric pressure gauges (PCB 113B24). The temperature and pressure behind the reflected shock wave were computed from the measured incident shock speed and the speed attenuation using a one-dimensional shock model. Derived from CO-absorption/emission measurements the

uncertainty in reflected shock temperature is estimated to be less than ±15 K in the temperature range of our measurements.

Ignition was observed by two methods. First, by measuring pressure profiles with piezoelectric gauges (PCB 113B24 and Kistler 603B) located at a distance of 10 mm to the end flange. Both pressure gauges were shielded by either 1 mm polyimide or RTV106 high temperature silicone rubber to reduce heat transfer and thus signal drift. Second, for determining ignition delay times, the CH* emission at 431 nm, at the same position ('radial') and through the end plate window ('axial'), was selected by narrow band pass filters (Hugo Anders, FWHM = 5 nm), detected with photomultipliers (HAMAMATSU R3896) and amplified by logarithmic amplifiers (FEMTO HLVA-100). All ignition delay time values shown in this paper were determined by measuring the time difference between the initiation of the system by the reflected shock wave at the end plate and the occurrence of the CH* maximum at the side port 10 mm away (figure 1 left). This allows for a good comparability to simulations. Furthermore, ignition delay times were corrected by an experimentally derived blast-wave propagation time delay and compared for validation at the highest temperatures within each series to the end plate emission characteristics. The experimental setup allowed measurements of ignition delay times up to 8 ms depending on the temperature and the gas mixture.

2.2 Laminar flame speed experiments

A high pressure burner system was used to measure the laminar flame speed of preheated C_2H_4 / N_2O gas mixtures diluted 1:2 with nitrogen. The experimental setup consists of the burner housing with the pressure control system, exhaust gas heat exchanger, the ignition system, and the flame holder. Calibrated Bronkhorst mass flow controllers were used for

regulating fuel, oxidizer, and diluent as well as the air co-flow. The gases were delivered by LINDE AG (N_2O: 99.95%, C_2H_4: 99.95%, diluent N_2: 99.999%). The flame holder is made of copper and heated to 473 K. Bulk temperature and gas temperature were monitored by type-K thermocouples. Contracting nozzles of different outlet diameters (1.5 to 8.0 mm) were used to stabilize the flame at different equivalence ratios and pressures. Typically, one change in nozzle diameter was sufficient to cover the complete range of fuel equivalence ratios at one pressure. Digital images of the flames were captured by a CCD camera (La Vision, Imager pro) in combination with a telecentric zoom lens (Navitar, 12x). From these images, contours and cone angles were calculated by using an edge detection algorithm. Figure 1 (right) provides a visual impression of a rich flame at ambient pressure without housing stabilized upon a contraction nozzle of Ø 6 mm in diameter.

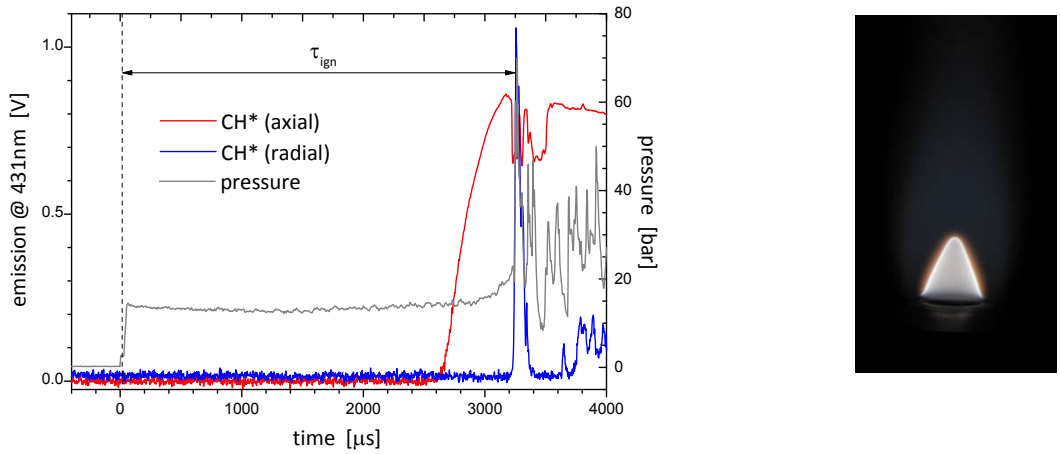

FIG. 1: (left) Pressure and emission profiles ('axial' – detected through the end plate window, 'radial' – detected through a side on window) for a stoichiometric 20% (C_2H_4 / N_2O) + 80% N_2 mixture at initial T = 1173 K and initial p = 13.7 bar; (right) Photography of a conical flame for 50% (C_2H_4 / N_2O) + 50% N_2 at $T_{preheat}$ = 473 K, ambient pressure, and an equivalence ratio of φ = 1.5 (nozzle diameter Ø 6 mm)

3. RESULTS AND MODELLING

Modelling of the ignition delay times was performed with an adapted version of CHEMKIN II (Kee et al. (1989)) with constant pressure option, whereas the laminar flame speed calculations were done with Cantera's 'Free Flame' model (Goodwin et al. (2016)). For a better comparison with model predictions, the GRI 3.0 from Smith et al. (2000) has been further extended with respect to the excited species OH* and CH* as proposed by Smith et al. (2002) and Kathrotia et al. (2012). Thus, the time of maximum [CH*] has been defined as 'ignition delay time', i.e. $\tau_{ign} = t([CH^*]_{max})$. Next, collision enhancement factors (CEF) for C_2H_4 and N_2O have been estimated to $CEF(C_2H_4) = CEF(C_2H_6)$ and $CEF(N_2O) = CEF(CO_2)$ and supplement all reactions with collisional partners involved. The reactions proposed by Powell et al. (2009) were added and high temperature dissociation reactions for N_2, NO, and CO completed the modification. Within the present work, this adapted mechanism is denoted as 'GRI3.0(adapted)'. The performance of this reaction model with respect to the ignition delay times, as shown in figure 2 (left), reveals largest deviations at an initial pressure of p = 1 bar. Deviations at lower temperatures, i.e. at longer ignition delay times, and at higher pressures are promoted by post-shock compression effects due to the attenuation of the reflected shock front interacting with the boundary layer. Figure 2 (right) shows the comparison between laminar flame speed calculations and measurements. The experimentally measured laminar flame speed is not decreasing with increasing pressure for p = 6 and 10 bar because heat transfer to the rim of the burner nozzel's exit seems to increase the preheat temperature beyond 473K. Bulk temperature did not indicate this deviation. Nevertheless, the characteristics of the profile $S_u(\varphi)$ in figure 2 (right) is reproduced fairly well. Test calculations with comprehensive reaction mechanisms including detailed hydrocarbon and nitrogen-chemistry as from the CRECK modelling group (2016) revealed even lower laminar flame speeds than using 'GRI3.0(adapted)'. Although diluted 1:2 with nitrogen, the

maximum flame temperatures exceed 2700 K easily. Especially the nitrogen thermodynamics and chemistry, predominantly validated at lower temperatures, shows a significant influence on the flame speed.

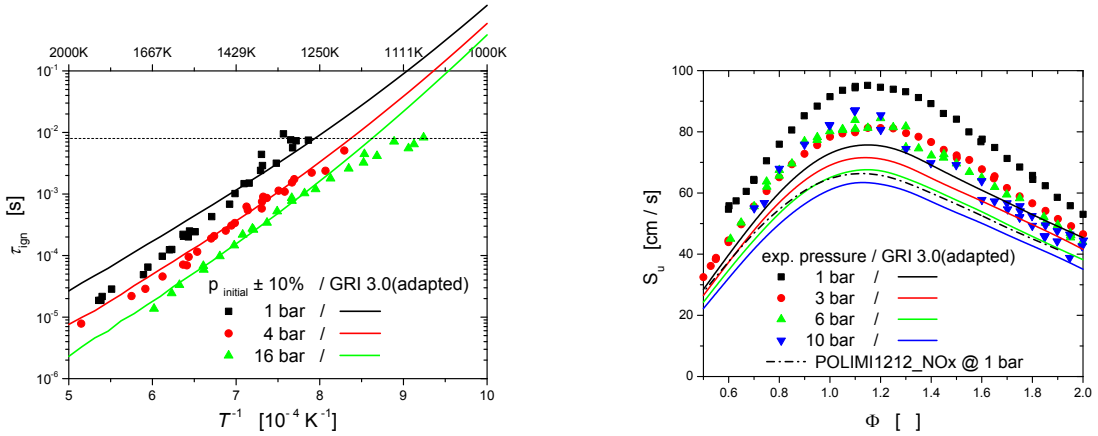

FIG. 2: (left) Ignition delay times for 20% (C_2H_4 / N_2O) + 80% N_2 at φ = 1.0 (symbols) and predictions of the 'GRI3.0(adapted)' mechanism calculated for p = const. conditions (lines); the dashed horizontal line indicates the limit of observation period. (right) Measured (symbols) and calculated (lines) laminar flame speeds for 50% (C_2H_4 / N_2O) + 50% N_2 at an unburned gas preheat temperature of $T_{preheat}$ = 473 K and different pressures compared to 'GRI3.0(adapted)' predictions. Scatter for different measurement series at p = 10 bar is mainly caused by the limits of flame stabilization.

In addition, a linear transformation model (linTM) developed by Methling et al. (2016) for the optimization and reduction of chemical kinetic models has been applied to a subset of nitrogen reactions and to the collision enhancement factor of N_2O, as explained in the following. Ignition delay time measurements at all pressures and laminar flame speed measurements at p = 1 bar have been selected as optimization targets. Note that this optimization is not meant as a 'determination' of reaction rate coefficients of elementary reactions targeting global observables, although the sensitivity to reactions R_1: N_2O (+N_2) →

N_2 + O (+N_2) and R_2: N_2O + H → N_2 + OH is overwhelming, but as a fit to the experimental data within the published error bounds of the respective reaction. In figure 3, the different reaction rates of R_1 and R_2 are compared to demonstrate the adjustments due to optimization.

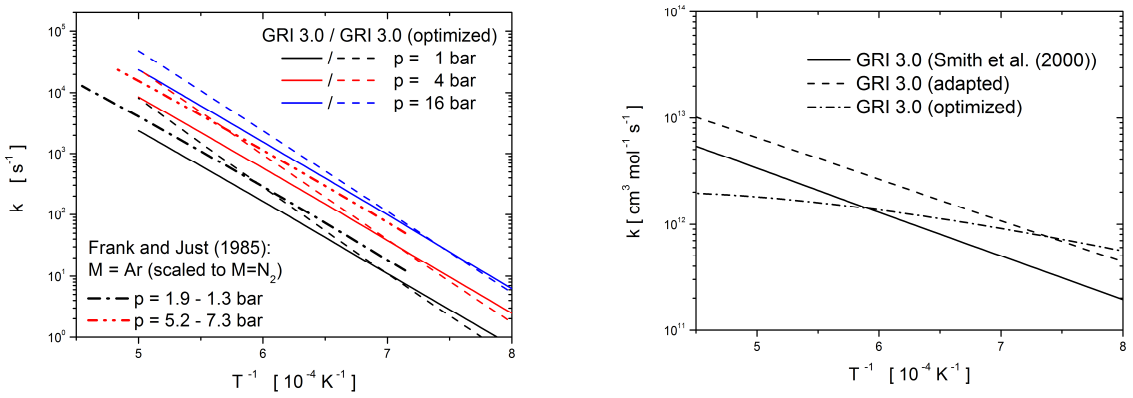

FIG. 3: (left) Reaction rates k(*T*,*p*;M) of R_1: N_2O (+N_2) → N_2 + O (+N_2) – original GRI 3.0 (Smith et al. (2000)) and 'GRI3.0(optimized)' version – compared to k(*T*) from Frank and Just (1985) scaled to N_2; (right) Reaction rates of R_2: N_2O + H → N_2 + OH.

For comparison, figure 3 (left) shows the result of a distinct experimental series of N_2O (+Ar) – decomposition measurements in two pressure regimes by Frank and Just 1985 as an example for the rate coefficients particularly with regard to the results of the optimization.

Besides R_1 and R_2, reactions R_3: N2O+H → NH+NO, R_4: H+NO+M → HNO+M and R_5: HNO+H → H2+NO have also been included in the optimization. The results are illustrated in figure 4 labelled as 'GRI3.0(optimized)'. Comparing figure 4 left to figure 2 left, the apparent activation energy of the reactive system at p = 1 bar agrees better with the one deduced from the measurements. Also, laminar flame speed measurements — only an optimization target for p = 1 bar — are reproduced sufficiently well. Varying the preheat temperature using the 'GRI3.0(optimized)' version, the estimated additional preheat temperature increase in figure 2 right was estimated to be 30 K @ φ = 0.5 rising to 60 K @ φ

= 1.5 at p = 6 bar, and 60 K @ φ = 0.5 rising to 90 K @ φ = 1.5 at p = 10 bar, resp. The fitted collision enhancement factor for N_2O in R_1 was determined to be 2.8.

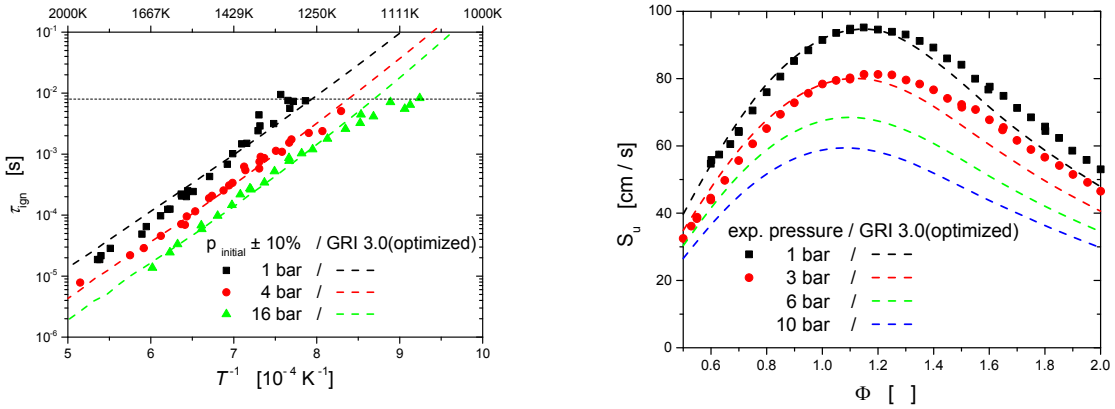

FIG. 4: (left) Ignition delay times (optimization target) for 20% (C_2H_4 / N_2O) + 80% N_2 at φ = 1.0 calculated with the optimized GRI3.0 mechanism version; (right) Laminar flame speed measurements for 50% (C_2H_4 / N_2O) + 50% N_2 at $T_{preheat}$ = 473 K and p = 1 bar (optimization targets) and p = 3 bar plus predictions for elevated pressures of this measurement series.

3. CONCLUSIONS AND SUMMARY

Ignition delay times and laminar flame speeds have been measured in nitrogen diluted C_2H_4/N_2O – mixtures at ambient and elevated pressures. The GRI 3.0 reaction model has been adapted with respect to collision enhancement factors and, amongst others, within a subset of sensitive nitrogen reactions like $N_2O + H \rightarrow NH + NO$ and $N_2O + H \rightarrow N_2 + OH$. Despite of this, predictive capability with respect to laminar flame speed measurements remained poor. Therefore, a linear transformation model for optimization was applied to this 'GRI3.0(adapted)' version. The result with respect to the defined targets (all ignition delay time measurements and laminar flame speeds only at p = 1 bar) is sufficiently good, so that improvement of the gas phase reaction mechanism is the next step towards CFD model combustor simulations. In addition, further investigations on high temperature hydrocarbon /

nitrous oxide reaction systems and species are recommended to improve our knowledge on the elementary reaction kinetics and thermodynamics involved.

ACKNOWLEDGMENTS

The authors thank Juan Ramon Diaz Moralejo, Abhishek Verma, Alexander Vollmer, and Bhaskar Bhatia for their support carrying out the experiments.

REFERENCES

Tiliakos, N., Tyll, J.S., Herdy, R., Sharp, D., Moser, M., and Smith, N., (2001) Development and Testing of a Nitrous Oxide / Propane Rocket Engine, AIAA-2001-3258.

ADMG (AEROSPACE DEFENSE MEDIA GROUP), Intelligent Aerospace, (2012) ALASA (Airborne Launch Assist Space Access): DARPA works with five aerospace companies to develop inexpensive launch capability for small satellites, URL: http://www.intelligent-aerospace.com/articles/2012/06/darpa_works_withfiveaerospacecompaniestodevelopinexpensivelaunch.html (accessed 2018/08/14).

Werling, L., Hochheimer, B., Baral, A., Ciezki, H., and Schlechtriem, S., (2015) Experimental and Numerical Analysis of the Heat Flux Occurring in a Nitrous Oxide / Ethene Green Propellant Combustion Demonstrator, AIAA 2015-4061.

Werling, L., Hauck, A., Mueller, S., Ciezki, H., and Schlechtriem, S., (2016) Pressure Drop Measurement of Porous Materials: Flashback Arrestors for a N2O / C2H4 Premixed Green Propellant, AIAA 2016-5094.

Werling, L., Lauck, F., Freudenmann, D., Röcke, N., Ciezki, H., and Schlechtriem, S., (2017) Experimental Investigation of the Flame Propagation and Flashback Behavior of a Green Propellant Consisting of N_2O and C_2H_4, J. Energy and Power Engineering, **11**, pp. 735-752.

Smith, G.P., Golden, D.M., Frenklach, M., Moriarty, N.W., Eiteneer, B., Goldenberg, M., Bowman, C.T., Hanson, R.K., Song, S., Gardiner, W.C. Jr., Lissianski, and V.V., Qin, Z., (2000) Gas Research Institute, URL: http://www.me.berkeley.edu/gri_mech/ (accessed 2018/08/14).

Powell, O.A., Papas, P., Dreyer, C., (2009) Laminar burning velocities for hydrogen-, methane-, acetylene, and propane-nitrous oxide flames, Comb.Sci.Tech., **181**, pp. 917-936.

Methling, T., Braun-Unkhoff. M., and Riedel, U., (2017) A novel linear transformation model for the analysis and optimisation of chemical kinetics, Combustion Theory and Modelling, **21**(3), pp. 503–528, DOI: 10.1080/13647830.2016.1251616.

Kee, R.J., Rupley, F.M., and Miller, J.A., (1989) Chemkin-II: A Fortran chemical kinetics package for the analysis of gas-phase chemical kinetics, Report No. SAND89-8009, Sandia National Laboratories.

Goodwin, D.G., Moffat, H.K., and Speth, R.L., (2016) Cantera: An object-oriented software toolkit for chemical kinetics, thermodynamics, and transport processes (version 2.2.1), URL: http://www.cantera.org (last access 2018/08/14).

Smith, G.P., Luque, J., Chung, P., Jeffries, J.B., and Crosley, D.R., (2002) Low Pressure Flame Determinations of Rate Constants for OH(A) and CH(A) Chemiluminescence. Combustion and Flame, **131**, pp. 59-69.

Kathrotia, T., Riedel, U., Seipel, A., Moshammer, K., and Brockhinke, A., (2012) Experimental and numerical study of chemiluminescent species in low-pressure flames, Applied Physics B, **107** (3), pp. 571 – 584, DOI: 10.1007/s00340-012-5002-0.

The CRECK Modeling Group, Politecnico di Milano: POLIMI_TOT1212NOx and references therein (2016), URL: http://creckmodeling.chem.polimi.it/index.php/menu-kinetics/menu-kinetics-detailed-mechanisms/menu-kinetics-complete-mechanism (accessed 2018/08/14).

Frank, P., and Just, Th., (1985) High Temperature Reaction Rate for $H+O_2=OH+O$ and $OH+H_2=H_2O+H$, Berichte d. Bunsengessellschaft f. physikalische Chemie, **89**, pp. 181-187.

FIGURE CAPTION

FIG. 1: (left) Pressure and emission profiles ('axial' – detected through the end plate window, 'radial' – detected through a side on window) for a stoichiometric 20% (C_2H_4 / N_2O) + 80% N_2 mixture at initial T = 1173 K and initial p = 13.7 bar; (right) Photography of a conical flame for 50% (C_2H_4 / N_2O) + 50% N_2 at $T_{preheat}$ = 473 K, ambient pressure, and an equivalence ratio of φ = 1.5 (nozzle diameter Ø 6 mm)

FIG. 2: (left) Ignition delay times for 20% (C_2H_4 / N_2O) + 80% N_2 at φ = 1.0 (symbols) and predictions of the 'GRI3.0(adapted)' mechanism calculated for p = const. conditions (lines); the dashed horizontal line indicates the limit of observation period. (right) Measured (symbols) and calculated (lines) laminar flame speeds for 50% (C_2H_4 / N_2O) + 50% N_2 at an unburned gas preheat temperature of $T_{preheat}$ = 473 K and different pressures compared to 'GRI3.0(adapted)' predictions. Scatter for different measurement series at p = 10 bar is mainly caused by the limits of flame stabilization.

FIG. 3: (left) Reaction rates k(T,p;M) of R_1: N_2O (+N_2) → N_2 + O (+N_2) – original GRI 3.0 (Smith et al. (2000)) and 'GRI3.0(optimized)' version – compared to k(T) from Frank and Just (1985) scaled to N_2; (right) Reaction rates of R_2: N_2O + H → N_2 + OH.

FIG. 4: (left) Ignition delay times (optimization target) for 20% (C_2H_4 / N_2O) + 80% N_2 at φ = 1.0 calculated with the optimized GRI3.0 mechanism version; (right) Laminar flame speed measurements for 50% (C_2H_4 / N_2O) + 50% N_2 at $T_{preheat}$ = 473 K and p = 1 bar (optimization targets) and p = 3 bar plus predictions for elevated pressures of this measurement series.